Available online at www.sciencedirect.com
SCIENCE DIRECT
Biochimica et Biophysica Acta 1708 (2005) 393 – 403
BIOCHIMICA ET BIOPHYSICA ACTA
BBA
http://www.elsevier.com/locate/bba

Oligomerization of H^+-pyrophosphatase and its structural and functional consequences

Hisatoshi Mimura, Yoichi Nakanishi, Masayoshi Maeshima*

Laboratory of Cell Dynamics, Graduate School of Bioagricultural Sciences, Nagoya University, Nagoya 464-8601, Japan

Received 10 March 2005; received in revised form 18 April 2005; accepted 10 May 2005
Available online 31 May 2005

Abstract

The H^+-pyrophosphatase (H^+-PPase) consists of a single polypeptide, containing 16 or 17 transmembrane domains. To determine the higher order oligomeric state of *Streptomyces coelicolor* H^+-PPase, we constructed a series of cysteine substitution mutants and expressed them in *Escherichia coli*. Firstly, we analyzed the formation of disulfide bonds, promoted by copper, in mutants with single cysteine substitutions. 28 of 39 mutants formed disulfide bonds, including S545C, a substitution at the periplasmic side. The formation of intermolecular disulfide bonds suppressed the enzyme activity of several, where the substituted residues were located in the cytosol. Creating disulfide links in the cytosol may interfere with the enzyme's catalytic function. Secondly, we prepared double mutants by introducing second cysteine substitutions into the S545C mutant. These double-cysteine mutants produced cross-linked complexes, estimated to be at least tetramers and possibly hexamers. Thirdly, we co-expressed epitope-tagged, wild type, and inactive mutant H^+-PPases in *E. coli* and confirmed the formation of oligomers by co-purifying one subunit using the epitope tag used to label the other. The enzyme activity of these oligomers was markedly suppressed. We propose that H^+-PPase is present as an oligomer made up of at least two or three sets of dimers.

Keywords: Disulfide bond; H^+-pyrophosphatase; Oligomerization; Proton pump

1. Introduction

H^+-translocating inorganic pyrophosphatase (H^+-PPase) uses inorganic pyrophosphate (PP_i) as an energy source to transport protons across biomembranes, generating electrochemical proton gradients for active secondary transport systems [1]. H^+-PPases, which consist of single polypeptides of about 80 kDa, form a unique protein family distinct from P-, F-, and V-type H^+-ATPases [2–4]. Their primary sequences differ from other H^+-pumps and soluble PPases, although they share a few functional motifs with the soluble PPases and P-type ATPases [2,4,5].

H^+-PPases are found in higher plants [4], parasitic and free-living protozoa [6,7], some eubacteria [8–10], and archaebacteria [3,11]. In these organisms, H^+-PPase acidifies intracellular organelles, such as vacuoles in plants [4], and acidocalcisomes in protozoa [12] and bacteria [13], together with V-ATPase. Recently, H^+-PPase has been suggested to exist in the yolk granule membrane of the insect, *Rhodnius prolixu* [14]. One of the physiological roles of H^+-PPase is to compensate for V-ATPase under conditions of energy stress [1]. In the photosynthetic bacterium *Rhodospirillum rubrum*, the transcription of H^+-PPase has been shown to increase in anaerobic conditions and increasing salt stress but decrease in aerobic conditions, under the control of its promoter [15]. Analysis of a null mutant in *R. rubrum* showed that this enzyme is not essential, but plays an important role in growth under low energy conditions such as low light intensity [16]. In plants, salt and osmotic stress are known to enhance the transcription of H^+-PPase [17] and its over-expression confers

Abbreviations: H^+-PPase, H^+-translocating pyrophosphatase; PP_i, inorganic pyrophosphate; ScPP, *S. coelicolor* H^+-PPase; BM, 3-(*N*-maleimidylpropionyl)biocytin; CuPh, Cu(II)-(1,10-phenanthroline)$_3$; DTT, dithiothreitol; 2-ME, 2-mercaptoethanol; ECL, enhanced chemiluminescence

* Corresponding author. Tel./fax: +81 52 789 4096.
E-mail address: maeshima@agr.nagoya-u.ac.jp (M. Maeshima).

0005-2728/$ - see front matter © 2005 Elsevier B.V. All rights reserved.
doi:10.1016/j.bbabio.2005.05.004

salt tolerance in a salt-sensitive yeast mutant [18] and tolerance to salt and drought in transgenic *Arabidopsis* plants [19]. Another function of this enzyme is to scavenge cytoplasmic PP_i, which is produced as a byproduct of various metabolic processes [1].

As well as the physiological role of H^+-PPase, the coupling mechanism between PP_i hydrolysis and active H^+ transport has also been studied. H^+-PPases strictly require Mg^{2+}, both for enzyme function and structural stabilization [20,21], but have been subdivided into two groups according to their K^+ requirements and their amino acid sequences [3]. Type I enzymes require at least 30 mM K^+ to be active [1] whereas Type II enzymes are fully active in the absence of K^+ [11,22]. Mutagenesis and antibody studies have identified functional residues and motifs in both types of H^+-PPase [5,23–30]. The presence of lysine rather than alanine residues in the conserved GNTT(K/A) motif has been proposed as a useful criterion to distinguish Type I and II enzymes, respectively [31]. Recently, Glu^{197} and Glu^{202} in *R. rubrum* H^+-PPase were shown to be involved in substrate binding, and Glu^{550} and Glu^{649} were demonstrated to be important for the correct folding of the polypeptide [32].

Although many functional residues have been reported, information about the tertiary structure of H^+-PPase is limited by the general difficulty of crystallizing membrane proteins. Most H^+-PPases contain 16 transmembrane domains with conserved motifs in their cytoplasmic loops [33]. Several groups have proposed that the functional unit for H^+-PPases is a dimer [1], on the basis of chemical cross-linking studies [34], gel filtration chromatography [35,36], radiation inactivation [35–37], inactivation by high hydrostatic pressure [38], and thermo-inactivation [39] using plant enzymes.

To determine which residues in the hydrophilic loops are involved in oligomerization, we have constructed a series of mutant enzymes, expressed them in *E. coli* and analyzed oligomer formation by cross-linking cysteine residues. In this study, we have focused on *S. coelicolor* H^+-PPase (ScPP), which can be functionally expressed in *E. coli.* We produced a series of site-directed mutants, substituting cysteines for single residues within the ScPP protein, and looked at the formation of disulfide bonds between the subunits. Studies using site-directed thiol cross-linking have provided insights into the structure of several other membrane proteins including the Na^+/H^+ exchanger [40,41], the metal-tetracycline/H^+ antiporter [42], lactose permease [43], mannitol permease [44], the multidrug transporter [45], and P-glycoprotein [46]. We have applied this method to ScPP to identify neighboring residues within oligomeric forms and to evaluate the biochemical implications of oligomerization. In addition, we constructed two epitope-tagged forms of ScPP, an active wild-type ScPP and an inactive ScPP mutant. Purification of these hetero-oligomeric enzyme complexes allowed us to confirm the association of multiple polypeptides in the bacterial membrane and to study the effect of oligomerization on enzyme activity. This study provides insights into the functional oligomerization and the structure–function relationship of H^+-PPases in membranes.

2. Materials and methods

2.1. Plasmid construction and site-directed mutagenesis

Substitution mutants of ScPP, in which individual cysteine residues or all cysteine residues were changed, were generated from a ScPP gene (sScPP), synthesized previously [33]. The sScPP gene was identical to the native enzyme (DDBJ/GenBank™/EBI accession number AB180905) with the exception of the substitution of Phe for Ser^{282}. ScPP proteins were expressed in plasmid pYN309 which was constructed from pET23b (Novagen) by modifying the *Pst*I site. A His_6-tagged cysteine-less ScPP (C-less-His) was generated from the expression plasmid pYN316, which encodes a His_6-tagged ScPP (ScPP-His), by substituting the four endogenous cysteine residues as follows: C178S, C179S, C253A, and C621V. Single cysteine substitutions were generated from a plasmid containing C-less-His (pHM17). Double cysteine mutants were generated from a plasmid that already contained the S545C substitution (pHM45). The plasmid vectors pET-Duet-1 and pCDFDuet-1 (Novagen) were used to co-express the native ScPP gene (nScPP) and sScPP. The original tags in these vectors were exchanged for a His_6-tag (pDuet-M2-His_6) and a FLAG epitope (pCDF-M2-FLAG), respectively, by PCR. The nScPP gene was amplified from the chromosomal DNA of a laboratory strain of *S. coelicolor* by PCR with KOD Dash DNA polymerase (Toyobo Co., Osaka, Japan) and inserted into the *Nde*I and *Xho*I sites of pCDF-M2-FLAG, to construct the expression plasmid (pHM99) for FLAG-tagged ScPP (ScPP-FLAG). sScPP was transferred from pYN316 to the *Nde*I and *Xho*I sites of pDuet-M2-His_6 to prepare a plasmid (pHM93) expressing ScPP-His. The pHM93 plasmid was used as a template to generate four mutants of ScPP-His ($S263C_w$, $S402C_w$, $S609C_w$, and $S694C_w$). Mutagenesis was carried out using a QuickChange site-directed mutagenesis kit (Stratagene) using the method of Kirsch and Joly [47]. All PCR-amplified products were sequenced to confirm the correct mutations were present.

2.2. Protein expression in E. coli and crude membrane preparation

Proteins were expressed in *E. coli* and crude membranes were prepared as previously described [33], but with slight modifications. *ScPP* constructs derived from plasmid pYN309 were introduced into the *E. coli* strain BLR(DE3)-pLysS K128I [33]. Transformants were selected in Luria–Bertani plates containing 50 μg/ml ampicillin and 34 μg/ml chloramphenicol. Expression vectors derived from pDuet-M2-His_6 and pCDF-M2-FLAG were introduced into the

E. coli strain BLR(DE3) (Novagene) and selected with 50 μg/ml ampicillin (pDuet-M2-His_6 derivatives) or 50 μg/ml spectinomycin (pCDF-M2-FLAG derivatives). Cells derived from single transformant colonies were grown for 16 h at 37 °C in Luria–Bertani medium supplemented with antibiotics and then diluted 50-fold in the same medium. After a further 4 h at 37 °C, isopropyl-1-thio-β-D-galactopyranoside was added to a final concentration of 0.4 mM (for the pYN309 derivatives) or 1 mM (for the pDuet-M2-His_6 and pCDF-M2-FLAG derivatives). After 2 h, the cells were disrupted by sonication, centrifuged, and the crude membranes were suspended in 10 mM Mes/Tris, pH 7.2, 0.15 M sucrose, 1 mM $MgCl_2$, and 75 mM KCl.

2.3. BM labeling assay

The binding abilities of cysteine-less and single-cysteine substitution mutants of ScPP-His, expressed in the *E. coli* strain BLR(DE3)pLysS K128I, were tested using BM (Molecular Probes), with intact cells, as described previously [33]. After labeling with BM, crude membrane fractions were prepared, the His-tagged proteins were solubilized from the membrane, purified, separated on SDS-PAGE in the presence or absence of 5% 2-ME, and then transferred to polyvinylidene difluoride membranes (Millipore). Biotinylated proteins were detected using a streptavidin-biotinylated horseradish peroxidase and ECL (Amersham Biosciences). Blots were stripped with 100 mM 2-ME and 62.5 mM Tris/HCl (pH 8.0) at 50 °C for 30 min and then re-probed with anti-H^+-PPase antibody [25] for immunoblotting.

2.4. Disulfide intermolecular cross-linking

Crude membranes prepared from BLR(DE3)pLysS K128I cells expressing ScPP-His cysteine mutants were suspended at 0.5–1.0 mg/ml protein in a buffer containing 10 mM Mes/Tris (pH 7.2), 0.15 M sucrose, 1 mM $MgCl_2$, 75 mM KCl, and 0.2 mM CuPh. After 20 min at 30 °C, the reaction was stopped by adding 25 mM Tris/HCl (pH 6.8), 5% SDS, 15% glycerol, 0.2% bromophenol blue, 20 mM EDTA, and 5 mM *N*-ethylmaleimide. Samples were subjected to SDS-PAGE and immunoblotting.

2.5. Immunoblotting

Proteins were separated by SDS-PAGE on 10% gels, and transferred to polyvinylidene difluoride membranes using a semidry blotting apparatus (BioRad). Three antibodies were used for immunoblotting: ScPP was detected with a rabbit polyclonal antibody against a conserved peptide motif, DVGADLVGKVEC [25]; His_6 tags in the expressed proteins were detected with polyclonal antibodies to His_6-tag (MBL Co., Nagoya, Japan) and FLAG epitope were detected with an anti-FLAG monoclonal antibody (Sigma). Antigens were visualized by the ECL method with an appropriate secondary antibody or with horseradish peroxidase-linked protein A (Amersham Biosciences).

2.6. Affinity purification and size-exclusion chromatography

Crude membranes treated with CuPh were washed with 50 mM Tris/HCl (pH 7.5), 20% glycerol, 300 mM KCl, 1 mM $MgCl_2$, 1 mM phenylmethanesulfonyl fluoride and 5 mM *N*-ethylmaleimide. The membrane vesicles were suspended in 50 mM Tris/HCl (pH 7.5), 20% glycerol, 300 mM KCl, 1 mM $MgCl_2$, 1% Triton X-100, 10 mM imidazole, and 5 mM *N*-ethylmaleimide. After centrifugation at 100,000×*g* for 15 min, the supernatant was mixed with Ni-nitrilotriacetic acid-agarose (Qiagen) and incubated for 1 h at 4 °C with gentle agitation. The agarose resin was pelleted and washed with 50 mM Tris/HCl (pH 7.5), 20% glycerol, 300 mM KCl, 1 mM $MgCl_2$, 1% Triton X-100, and 50 mM imidazole. Bound proteins were released with 50 mM Tris/HCl (pH 7.5), 20% glycerol, 300 mM KCl, 1 mM $MgCl_2$, 1% Triton X-100, and 200 mM imidazole. 0.1 μg aliquots of the eluate were mixed with 25 mM Tris/HCl (pH 6.8), 5% SDS, 15% glycerol, and 0.2% bromophenol blue, with or without 5% 2-ME, and subjected to SDS-PAGE. The remaining eluate was concentrated by spin-filtration with a Vivaspin tube (cutoff size, 50 kDa; Vivascience) and applied to a Superdex 200 HR 10/30 column (Amersham Biosciences) equilibrated with 20 mM Tris/HCl (pH 7.5), 10% glycerol, 150 mM KCl, 1 mM $MgCl_2$, and 0.1% *n*-dodecyl-β-D-maltoside. The eluate was collected in 1-ml fractions and subjected to immunoblotting.

2.7. Protein and enzyme assays

Protein concentrations, PP_i hydrolytic activity and PP_i-dependent H^+-transport activity were measured as described previously [33], but with slight modifications. In disulfide cross-linking experiments, the crude membrane fractions were treated with 0.2 mM CuPh and then diluted 100-fold to measure the PP_i hydrolytic activity. For H^+-transport assays, cell membranes were washed with 10 mM Mes/Tris (pH 7.2), 0.15 M sucrose, 1 mM $MgCl_2$, and 75 mM KCl and then incubated with 20 mM DTT in the same buffer for 20 min at 30 °C. As a control, membranes were treated with CuPh or DTT alone using the same procedure. In experiments co-expressing ScPP-His and ScPP-FLAG, the enzymes were assayed in the presence of 0.5 mM DTT.

3. Results

3.1. Spontaneous disulfide cross-linking of a single-cysteine mutant S545C

In our previous analysis of cysteine residues, which looked at the membrane topology of ScPP, one mutant enzyme with a single substitution, S545C, was not labeled

with BM [33], a membrane permeable sulfhydryl reagent. BM covalently binds to cysteine residues in hydrophilic regions but not in transmembrane domains and the hydrophobic space. Since Ser^{545} is located in the large loop *l*, which is exposed to the periplasm in the topological model of the enzyme (see Fig. 2), the above observation suggests that Cys^{545} in the S545C mutant is involved in the formation of a disulfide bond.

To test this possibility, we expressed the S545C mutant enzyme with a His_6 tag in *E. coli*, isolated the products from the cells, and then separated them by 10% SDS-PAGE with or without the reducing reagent 2-ME. Immunoblotting with anti-H^+-PPase antibodies showed the S545C mutant as a major band at around 150 kDa in the absence of 2-ME (Fig. 1, left panel), corresponding to the position of a dimer. Under reducing conditions, most of the 150-kDa band disappeared and a 72-kDa band appeared. The T552C mutant enzyme, which was partially biotinylated with BM, showed a similar pattern to S545C. Two other single-cysteine mutants, T497C and I605C, were biotinylated with BM and did not show the migration shift in the presence of 2-ME, indicating an absence of disulfide bonds. From these results, we concluded that the S545C mutant existed as a dimer in *E. coli* membranes, with Cys^{545} forming disulfide bonds and consequently, preventing biotinylation. This spontaneous disulfide cross-linking was not observed in the other single-cysteine mutants (data not shown), with the exception of T552C. Thr^{552} is located in the same loop, *l*, as

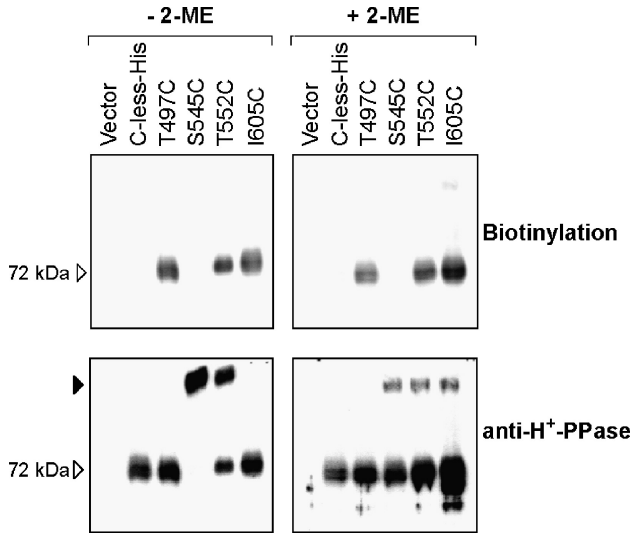

Fig. 1. Spontaneous disulfide bond formation in the single-cysteine ScPP mutant S545C inhibits biotinylation. *E. coli* cells expressing the empty vector (Vector), the cysteine-less ScPP-His (C-less-His), or the single-cysteine ScPP-His mutants were treated with BM. The reaction was stopped by adding buffer containing *N*-ethylmaleimide. ScPP proteins were isolated from the cells, separated by 10% SDS-PAGE with (+2-ME) or without (−2-ME) 2-ME, and transferred to a polyvinylidene difluoride membrane. The incorporated biotin was detected using the streptavidine biotinylated horseradish peroxidase complex (Biotinylation). The same blot was re-probed with anti-H^+-PPase antibody (ScPP-His). Open arrowheads indicate 72 kDa bands corresponding to monomers of ScPP-His. The black arrowhead indicates the oligomeric band.

Ser^{545}. It should be noted that all the mutant enzymes tested, including S545C and T552C, retained enzyme activity. The wild-type and mutant enzymes were recovered in the *E. coli* membrane fraction without aggregation or formation of inclusion bodies in cells.

3.2. Disulfide intermolecular cross-linking of cysteine mutants with copper

Observations on the S545C mutant led us to look at intermolecular disulfide cross-linking by other single-cysteine mutants. For this purpose, we made a series of single-cysteine mutants at 39 positions, covering all of the extramembrane loops, including the N- and C-termini. The predicted locations of these cysteine residues are shown in Fig. 2.

Membranes were prepared from *E. coli* expressing each of these mutant enzymes and treated with an oxidizing reagent, CuPh, to stimulate the formation of disulfide bonds. The oligomeric forms of the enzymes were analyzed on immunoblots with anti-H^+-PPase antibodies, on which most mutants showed bands at high molecular masses (Fig. 3A). ScPP proteins were electrophoresed as diffuse bands on SDS-PAGE like many other polytopic membrane proteins.

The efficiency of cross-linking and the electrophoretic mobility of the products varied with the mutant. Disulfide cross-linking was detected in 28 mutants (S7C, T15C, S52C, I56C, Q96C, T137C, S151C, I231C, T241C, A253C, S263C, R308C, S313C, A317C, T352C, S360C, S485C, T497C, S545C, T552C, I605C, L652C, S694C, T700C, T705C, S740C, S768C, and S787C), implying that these residues face each other in the homodimers. The other 11 mutants, such as S101C and D281C, did not form disulfide bonds.

In one mutant, L652C, the disulfide bond could not be completely reduced by 2-ME, even at high concentrations. We found that a hydrophobic reducing reagent, ethanedithiol, reduced the bond at 100 mM (Fig. 3B). These results indicate that Cys^{652} is located in a hydrophobic environment, as suggested from the topology of ScPP (Fig. 2).

Then, we examined a possibility of higher order oligomerization. For this purpose, we constructed double-cysteine mutants by introducing 14 of the 28 cysteine mutations, able to form disulfide bonds (Fig. 3A), into the S545C mutant. A spontaneous formation of disulfide bond between Cys^{545} residues occurred without CuPh as mentioned above. Thus, this disulfide bond may affect the interaction between additionally introduced cysteine residues. After treatment with CuPh, the corresponding single-cysteine mutants showed a band at around 150 kDa (Fig. 3C, left panel). Eight of the double mutants (S52C/S545C, S151C/S545C, I231C/S545C, S313C/S545C, S360C/S545C, S485C/S545C, I605C/S545C, and S787C/S545C) produced larger complexes about 290 and 440 kDa in addition to the 150-kDa complex (Fig. 3C, right panel), strongly suggesting that these double-cysteine mutants

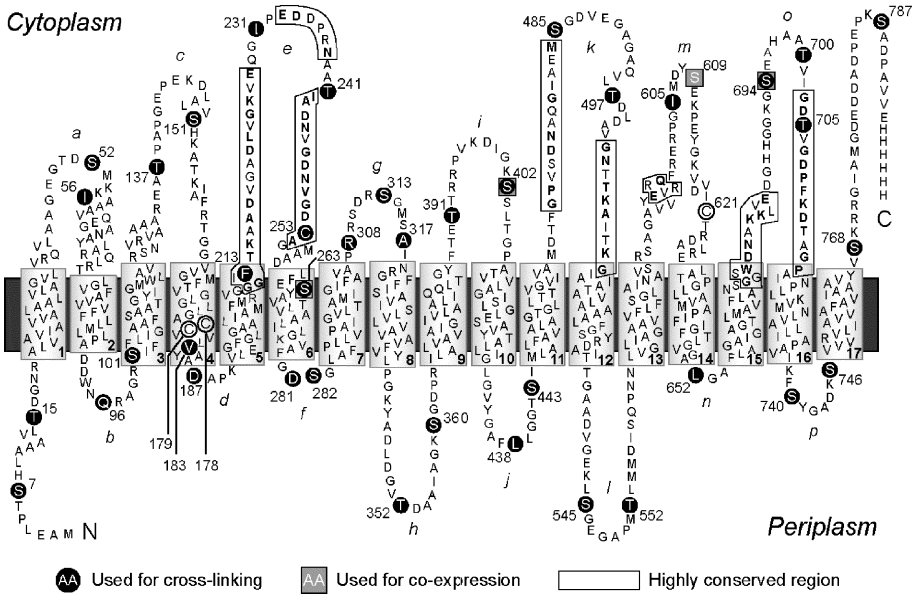

Fig. 2. Model showing the membrane topology of ScPP and the locations of introduced cysteines. This model is based on our previous study [33]. Conserved motifs such as GGIFTKAADVGADLVGKVE are boxed, and the residues common to various H^+-PPases are in boldface. The four endogenous cysteines (Cys^{178}, Cys^{179}, Cys^{253}, and Cys^{621}) are marked with circles. The 39 residues, such as Ser^{7}, Tyr^{15}, and Ser^{52}, which were replaced with cysteine in single-cysteine mutants, are indicated by black circles. The four residues (Ser^{263}, Ser^{402}, Ser^{609}, and Ser^{694}) replaced with cysteine in inactive ScPP-His mutants, which were used in the co-expression study, are indicated by gray squares. Six histidine residues shown at the C terminus represent the His_6 tag.

formed homo-dimers, tetramers, and hexamers after treatment with CuPh.

The remaining six double-cysteine mutants (S7C/S545C, Q96C/S545C, L652C/S545C, T700C/S545C, T705C/S545C, and S740C/S545C) showed only a single band at around 150 kDa, suggesting that these mutants formed only dimers, cross-linked by Cys^{545} or the other introduced cysteine residue. If the mutants formed intramolecular disulfide bonds, they would be expected to migrate as monomers. Since there was no band at 72 kDa (Fig. 3C, right panel), it was concluded that intramolecular cross-linking did not occur in this experiment.

3.3. Determination of the oligomeric state

The number of subunits making up the oligomeric complexes was estimated for five single-cysteine mutants (S545C, I605C, T700C, S740C, and S787C) and two double-cysteine mutants (I605C/S545C and S787C/S545C). Enzyme purification, using Ni-nitrilotriacetic acid-agarose, was an essential step for the analysis, because the enzyme is at a relatively low concentration within *E. coli* membranes (Fig. 4A). The purified ScPP preparations migrated at around 150 kDa in SDS-PAGE in the absence of 2-ME. In the presence of 2-ME, the 150-kDa bands disappeared and 72-kDa bands appeared (Fig. 4B), showing that the 150-kDa bands corresponded to dimeric forms of the ScPP-His proteins but not to complexes with other unidentified proteins.

When the purified preparations were subjected to size-exclusion chromatography on Superdex 200 HR (Fig. 4C), the wild-type and cysteine-less ScPP-His enzymes were eluted in fraction 14, which is the same fraction as that of the marker protein catalase (232 kDa). The detergent used in this experiment was *n*-dodecyl-β-D-maltoside with molecular weight of 510, critical micelle concentration of 0.17 mM, and aggregation number of 78 to 92 (40 to 47 kDa) (www.anatrace.com). The size of complex of the dimer of H^+-PPase and *n*-dodecyl-β-D-maltoside was estimated to be more than 200 kDa. Thus, we estimated that the size of the wild-type enzyme in fraction 14 was the H^+-PPase dimer associated with the detergent. All single-cysteine mutants (S545C, I605C, S740C, and S787C) were recovered in fractions 12 and 13, suggesting a larger complex of about 440 kDa, which may be a tetramer of ScPP. The double-cysteine mutants (I605C/S545C and S787C/S545C) eluted in fractions 10 to 12, equivalent to a still larger molecular weight of approximately 669 kDa, consistent with a hexamer of ScPP.

3.4. Effects of intermolecular disulfide cross-linking on the enzyme activity

We determined the enzyme activity of a series of single-cysteine mutants to see whether intermolecular cross-linking affected the enzyme activity of ScPP. Membrane vesicles containing mutant enzymes were treated with DTT or CuPh and then assayed for PP_i hydrolysis and PP_i-dependent H^+ transport. Oligomerization promoted by CuPh did not increase the activity of any of the mutant enzymes (Fig. 5). The C-less-His mutant retained activity after treatment with CuPh, indicating that this treatment had no effect on

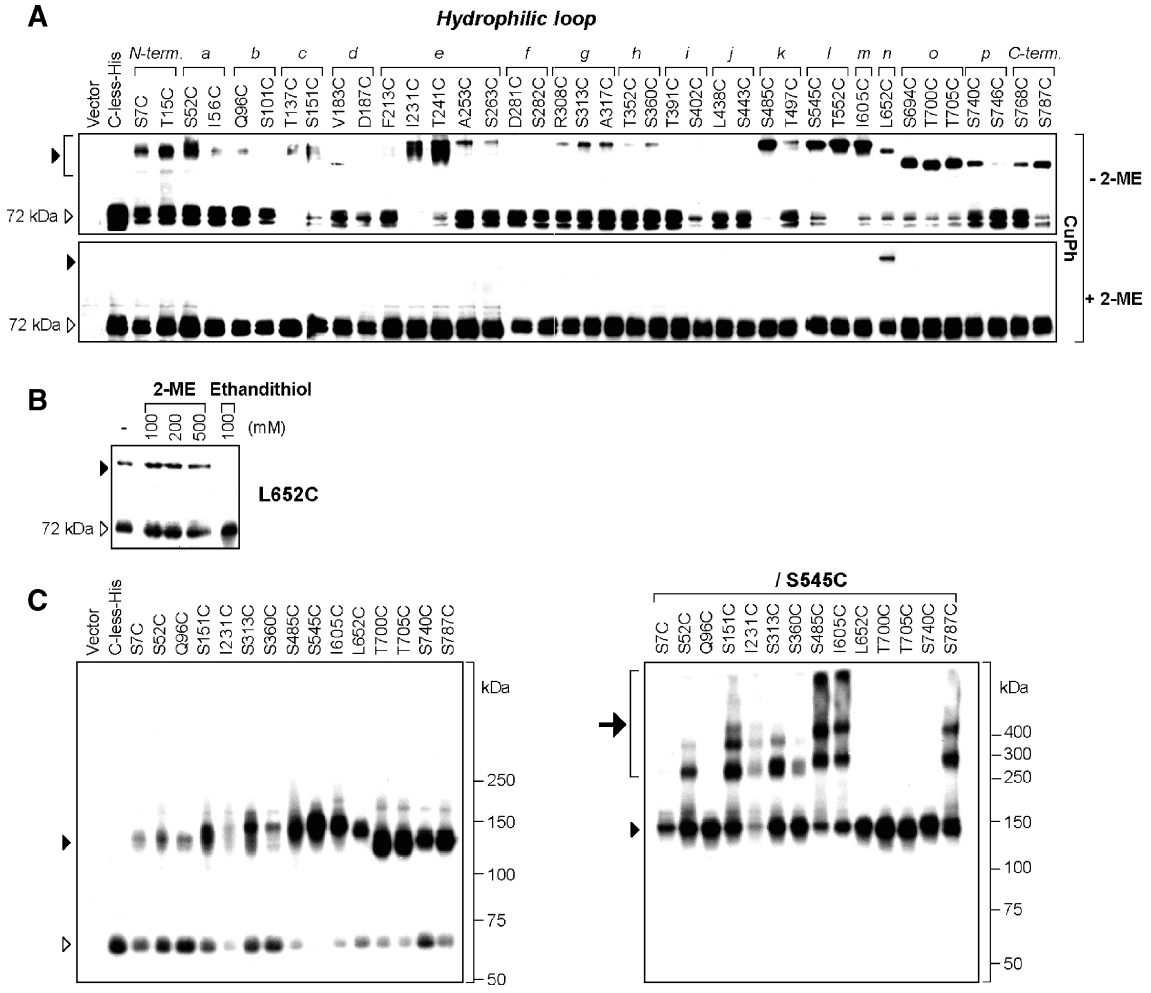

Fig. 3. Disulfide cross-linking of the cysteine mutants by CuPh. Crude membranes prepared from *E. coli* expressing cysteine mutants of ScPP-His were treated with 0.2 mM CuPh at 30 °C for 20 min. (A) Immunoblot of the *E. coli* membranes (5 μg) with anti-H^+-PPase antibody. Samples were separated by 10% SDS-PAGE with (+2-ME) or without (−2-ME) 2-ME. (B) Immunoblot of membranes (5 μg) containing the L652C mutant. Samples were reduced with 2-ME (+2-ME) or ethandithiol (Ethandithiol) at the indicated concentrations. (C) Immunoblot of membranes (10 μg) from ScPP-His mutants containing single (left panel) and double (right panel) cysteine substitutions with anti-H^+-PPase antibody. The double-cysteine mutants were generated by introducing the second cysteine residue into the S545C mutant at indicated positions. Samples treated with CuPh were separated by SDS-PAGE using 4–10% gradient gels under non-reducing conditions. The open triangle indicates bands corresponding to ScPP-His monomer. Closed triangles indicate bands corresponding to dimers and the arrow indicates bands corresponding to large oligomers. The figures on the ordinate indicate the scale used to estimate molecular masses. For further details, see Materials and methods.

ScPP enzyme activity in general. CuPh treatment markedly decreased both the PP_i-hydrolysis and H^+-transport activities of seven mutants (S151C, I231C, S313C, T391C, S485C, I605C, and T700C), although there was a recovery in activity after subsequent treatment with DTT (Fig. 5, CuPh + DTT). This result suggested that cross-linking these residues inhibits a conformational change occurring as part of the catalytic reaction of ScPP.

Other mutants retained more than 70% of their original activity after treatment with CuPh. There are two possible explanations for this result: (i) disulfide cross-linking did not occur in these mutants (see Fig. 2A; D187C, D281C, and S443C), or (ii) disulfide cross-linking did not affect the enzyme function in these other mutants (S7C, S52C, Q96C, S360C, S545C, L652C, S740C, S787C, and S787C/S545C).

3.5. Functional interaction of ScPP subunits in the membrane

To investigate the enzyme activity of heterodimers composed of active wild-type and non-functional mutant subunits in *E. coli* membranes, we co-expressed both subunits in *E. coli* using two compatible plasmids, pDuet-M2-His_6 and pCDF-M2-FLAG. We used His_6-tagged ScPP (ScPP-His) and FLAG-tagged ScPP (ScPP-FLAG) to distinguish the wild type and mutant subunits, and co-transformed *E. coli* cells with each pair of plasmids (ScPP-His/pCDF-M2-FLAG, pDuet-M2-His_6/ScPP-FLAG, or ScPP-His/ScPP-FLAG). Fig. 6A shows that anti-His_6-tag and anti-FLAG antibodies specifically distinguished the tagged ScPP chains in *E. coli* membranes and that both ScPP-His and ScPP-FLAG proteins accumulated in the membranes.

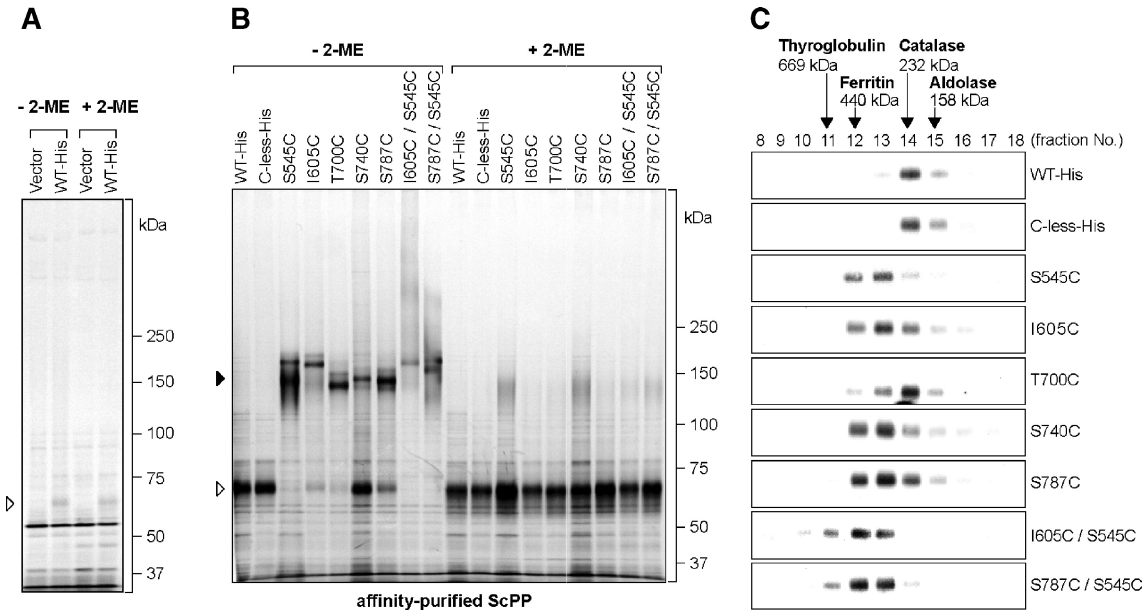

Fig. 4. Determination of the oligomeric states of single- and double-cysteine mutants oxidized with CuPh. (A) SDS-PAGE of *E. coli* membranes (0.1 μg) expressing empty vector (Vector) and wild-type ScPP-His (WT-His) on a 4–10% gradient gel under non-reducing (−2-ME) or reducing conditions (+2-ME). The gel was silver-stained. The open triangle indicates a band corresponding to ScPP-His monomer. (B) Membranes containing the wild-type ScPP-His, cysteine-less ScPP-His, and single- and double-cysteine ScPP-His proteins were treated with CuPh and solubilized with 1% Triton X-100. The His_6-tagged ScPP proteins were purified as described under the Materials and methods. Affinity-purified His_6-tagged proteins (0.1 μg) were separated by SDS-PAGE on a 4–10% gradient gel under non-reducing (−2-ME) or reducing conditions (+2-ME). Protein bands were visualized by silver staining. The open triangle indicates bands corresponding to ScPP-His monomer and the closed triangle indicates bands corresponding to the dimer. The arrow indicates bands corresponding to tetramers and larger complexes. (C) Size-exclusion chromatography of the purified ScPP on a Superdex 200 HR column. Eluted fractions (8 to 18) were analyzed by immunoblotting with anti-H^+-PPase antibody. Peak fractions containing molecular size markers (thyroglobulin, 669 kDa; ferritin, 440 kDa; catalase, 232 kDa; aldolase, 158 kDa) are indicated with arrows.

When the ScPP proteins were affinity purified with Ni-agarose, using the His_6-tag, from *E. coli* expressing both ScPP-FLAG and ScPP-His, and then used for immunoblotting, anti-FLAG antibodies labeled a band at the expected position (Fig. 6B). This co-purification clearly demonstrates a physical linkage between ScPP-His and ScPP-FLAG. To further examine the hetero-oligomers under relatively natural conditions, we substituted four individual residues (Ser^{263}, Ser^{402}, Ser^{609}, and Ser^{694}) in wild-type ScPP-His with cysteine; when we substituted these residues with cysteine in the C-less mutant, the enzyme was completely inactive [33]. The wild-type ScPP-His, the ScPP-His inactive mutants such as $S263C_w$, and the wild-type ScPP-FLAG were all detectable in *E. coli* membranes (Fig. 6C, left half). The co-expression of the ScPP-His inactive mutant and the ScPP-FLAG subunits was also confirmed (Fig. 6C, right half).

Two of the expressed mutants, $S402C_w$ and $S609C_w$, but not $S263C_w$ and $S694C_w$, retained both PP_i hydrolysis and H^+ transport activities (Figs. 6, D and E). When the wild type subunit of ScPP was co-expressed with different mutant subunits, there were no marked differences in the protein level (Fig. 6C). However, the PP_i hydrolysis and H^+ transport activities were markedly lower when the wild-type subunit was co-expressed with mutant subunits $S263C_w$ or $S694C_w$ compared to ScPP-His (Figs. 6D and E; right half). These suppressive effects were particularly clear when the activities were expressed relative to the amount of accumulated WT-FLAG protein (Figs. 6D and E; bottom columns). In these cases, the PP_i hydrolysis and H^+ transport activities were normalized to the amount of ScPP-FLAG. Thus, we concluded that the enzyme function was suppressed in hetero-oligomers formed between active and inactive subunits, i.e., the oligomerization of ScPP subunits had a negative effect on the enzyme function.

4. Discussion

The results of the disulfide cross-linking studies presented here clearly indicate that ScPP exists as oligomeric units. This study was prompted by the finding that the mutant enzyme with a single cysteine substitution at Ser^{545}, located in the periplasmic loop *l*, did not react with BM, a membrane permeable cysteine reagent. This S545C mutant formed homodimers with an efficiency of almost 100%, as shown by its failure to be biotinylated (Fig. 1). This result suggested that Cys^{545} in the S545C mutant was very close to another Cys^{545} in the homodimer. The disulfide bond is a so-called zero-length cross-linker. Based on the premise that cysteine cross-linking indicates the distance between two reactive cysteine residues, we infer that Ser^{545} faces another Ser^{545} in the wild-type oligomer. However, because proteins are subject to consid-

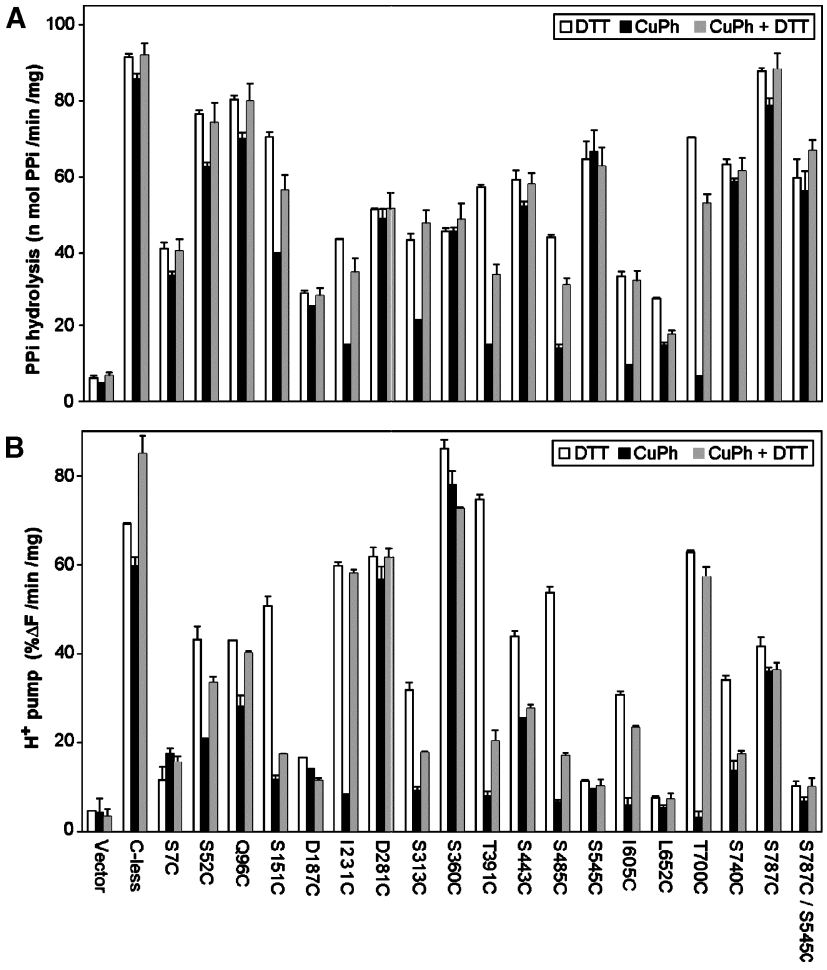

Fig. 5. Effect of disulfide cross-linking on ScPP function. (A) PP_i hydrolysis activity of cysteine mutants of ScPP-His. Membrane vesicles were treated with DTT (DTT) or CuPh (CuPh). In some cases, DTT was added after treatment with CuPh (CuPh + DTT). After chemical treatment, the suspensions were diluted 100-fold with buffer without DTT or CuPh. Enzyme assays were performed in the presence of 0.5 mM DTT unless CuPh treatment was used. (B) PP_i-dependent H^+-transport activity of membrane vesicles (250 μg). After treatment with DTT or CuPh, these reagents were removed by centrifugation of the vesicles and resuspension in a buffer without reducing and oxidizing agents. The data in A and B are presented as the mean ± standard deviation (S.D.) of triplicate and duplicate assays, respectively. For further details, see Materials and methods.

erable thermal motion, the interaction between residues and the stereochemistry of proteins cannot always be simply deduced from their chemical reactivity.

4.1. Cross-linking at cytoplasmic loops inactivated ScPP

Experiments using an oxidizing agent provided more detailed information about ScPP oligomerization. The present results suggest that cysteine substitutions at several positions in cytoplasmic loops can produce dimeric forms. Oligomerization of the single-cysteine mutants (S151C, I231C, S313C, T391C, S485C, I605C, and T700C) in cytoplasmic loops *c*, *e*, *g*, *i*, *k*, *m*, and *o* resulted in marked decrease in the PP_i-hydrolysis and H^+ transport activities, although each single-cysteine mutant regained enzyme activity following subsequent treatment with DTT. This inhibitory effect cannot be ascribed to chemical modification by copper since other mutants, such as S7C and S787C, were not affected. These results indicated that fixation of the cytoplasmic loops, especially loops *c*, *e*, *g*, *i*, *k*, *m*, and *o*, may have inhibited the binding of the substrate and/or conformational changes during catalysis.

All of these loops contain sequences conserved among H^+-PPases from various organisms, including GGIFTKAADVGADLVGKVE, EDDPRN, and IADNVGDNVGDCA (loop *e*, common residues are underlined), GPVSDNAQGIAEM and GNTTKAITKG (loop *k*), EVRRQ (loop *m*), and GGSWDNAKKLVE and GDTVGDPFKDTAGP (loop *o*) (2–4, 33). Three of these motifs (GGIFTKAADVGADLVGKVE, EDDPRN, and GDTVGDPFKDTAGP) have been demonstrated to form the catalytic site of H^+-PPases (5, 32). Moreover, two glutamate residues in Glu^{550}-VRRQ (loop *m*) and GGAWDNAKKYI-Glu^{649} (loop *o*) of the *R. rubrum* enzyme have been reported to be essential for folding to form the tertiary structure [32]. We propose that the H^+-PPase activity involves conformational changes affecting at least seven cytoplasmic loops; namely, four loops that

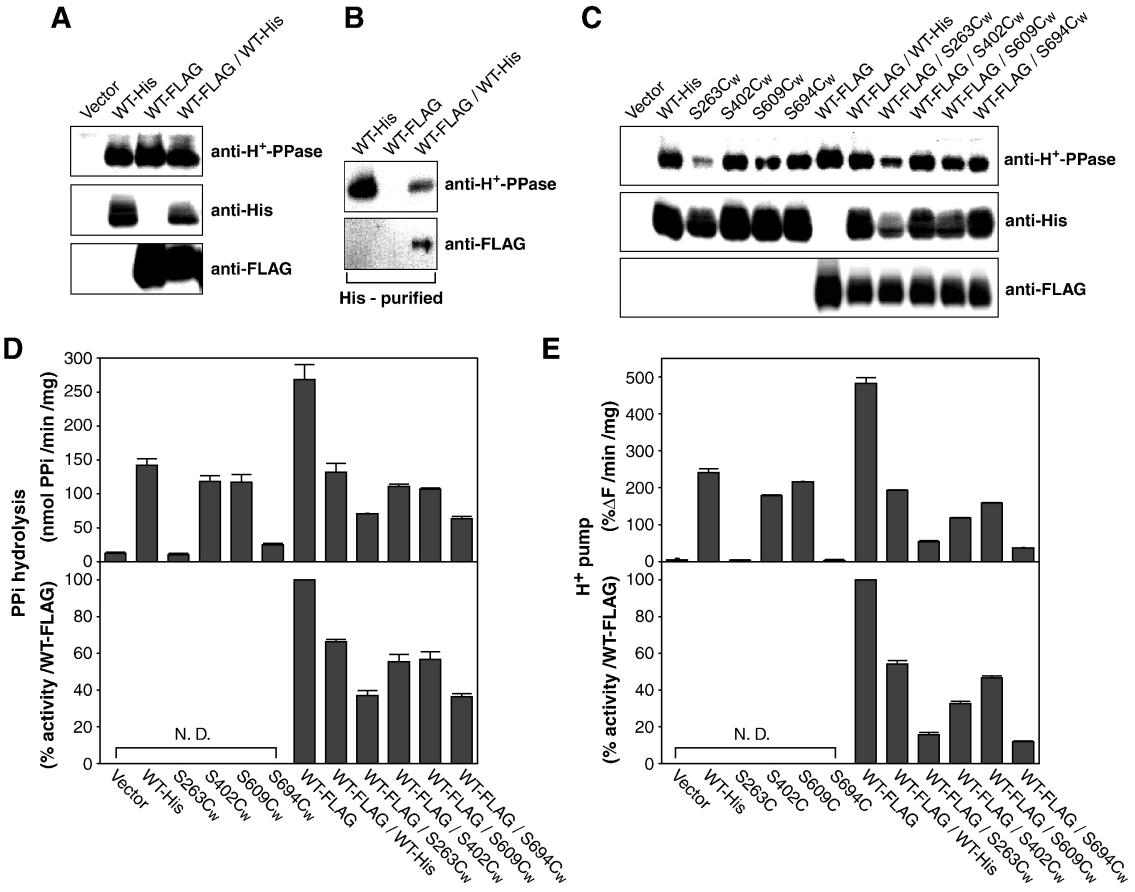

Fig. 6. Co-expression of the wild-type and inactive mutant form of ScPP affects the enzyme activity. (A) Immunoblot of membranes (10 μg) prepared from *E. coli* co-expressing wild-type ScPP-FLAG and ScPP-His mutant (WT-FLAG/WT-His) with anti-H^+-PPase (ScPP), anti-His-tag (His), and anti-FLAG antibodies (FLAG). (B) Co-purification of ScPP-FLAG with ScPP-His. Membranes from *E. coli* co-expressing ScPP-FLAG and ScPP-His mutant were solubilized with 1% Triton X-100 and then purified on Ni-nitrilotriacetic acid-agarose. The purified samples were analyzed by immunoblotting with anti-H^+-PPase and anti-FLAG antibodies. (C) Immunoblot of membranes co-expressing ScPP-FLAG and ScPP-His mutant with anti-H^+-PPase, anti-His-tag, and anti-FLAG antibodies. (D) PP_i hydrolysis activity of *E. coli* membranes. (E) PP_i-dependent H^+-transport activity of membrane vesicles (250 μg) prepared from *E. coli*. Activities relative to the amount of ScPP-FLAG are shown in the lower panels of D and E. The data are presented as the mean ± S.D. of triplicate and duplicate assays, respectively. N. D., not determined.

contain conserved motifs (*e*, *k*, *m*, and *o*) and three other loops (*c*, *g*, and *i*).

Other mutations in periplasmic loops (S7C, Q96C, S360C, S545C, L652C, and S740C) and at the C-terminus (S787C) produced dimeric forms but had no effect on function, suggesting that conformational changes do not occur in periplasmic domains. Recently, difference in the tertiary structure of Ca^{2+}-ATPase among catalytic states is clearly demonstrated at atomic level [48]. Ca^{2+}-ATPase shows drastic structural changes including the rearrangement of transmembrane helices. In contrast to Ca^{2+}-ATPase, the present study suggests that H^+-PPase may not show drastic rearrangement of periplasmic domains and transmembrane helices.

4.2. Negative effect of oligomerization with non-functional subunits

Co-expression of active subunits with inactive mutant subunits indicated the biochemical significance of ScPP oligomerization. Expressing the subunits with specific His_6 and FLAG tags confirmed this interaction and the formation of hetero-oligomers (Fig. 6). Interactions between the active and inactive subunits of ScPP resulted in decrease in the activity. Oligomers of the active wild-type subunit (ScPP-FLAG) with mutant subunits ($S263C_w$, $S402C_w$, $S609C_w$, and $S694C_w$) did not have full activity. In oligomers containing $S263C_w$ and $S694C_w$, the proton pump activities were 30% and 23%, respectively, of that of the combined, tagged wild-type subunits (ScPP-FLAG/WT-His) (Fig. 6E). These observations indicate that enzyme function is dependent upon subunit-subunit interaction.

Formation of dimers and higher order oligomers may stabilize the structure in the membranes and alter the functional properties. The functional significance of oligomerization has been discussed for several membrane transporters. In the case of the *E. coli* Na^+/H^+ antiporter, which has been proposed to exist as a homo-oligomer, intermolecular cross-linking changed the pH profile of the activity [49]. The serotonin transporter, which is a membrane

protein with 12 transmembrane domains, has been shown to form a tetramer by the association of dimers [50]. A functional consequence of this oligomerization has been demonstrated. Ludewig et al. [51] also reported that co-expression of wild-type and mutant proteins inhibited the activity of the tomato ammonium transporter.

Oligomerization of H^+-PPases may be related to allosteric functions, including the interactions with free magnesium and potassium ions, which are known cofactors for the enzyme [1,52]. The formation of higher order oligomers may also provide a possibility for scaffolding of the enzyme in the membrane in living cells.

4.3. Oligomerization and the interface

We suggest that ScPP forms oligomers in *E. coli* membranes based on the following findings: (i) the demonstration of interactions between the ScPP polypeptides in situ by the cross-linking of cysteine substitution mutants and the co-purification of nScPP-FLAG and His_6-tagged ScPP subunits; (ii) the detection of functional interactions between ScPP proteins. This study suggests the association of ScPP dimers into higher order complexes, based on the identification of cross-linked complexes from double-cysteine substitution mutants, migrating with molecular masses over 250 kDa in SDS-PAGE, where dimers migrated with a mass of 150 kDa (Fig. 3C). In addition, the cross-linked products from the mutants eluted as large complexes of 400 to 550 kDa in size-exclusion column chromatography, in which dimers behaved as about 230-kDa molecules (Fig. 4C), reflecting the size of oligomer–detergent complexes. Finally, we propose that ScPP has the potential to form tetramers and possibly hexamers, through the association of two dimers, in the membranes. We believe that stable dimers form the basic functional unit for this enzyme and that the individual dimer, within larger oligomers, functions independently. This idea is in agreement with previous findings that plant H^+-PPases also form oligomers and that their functional units are dimers [34–39].

In this study, we have identified some of the residues located in the interface between oligomers. Residue Ser^{545}, located in the periplasmic space, is strongly implicated as forming part of the interface between the subunits, since the S545C mutant formed a dimer without CuPh treatment and retained enzyme activity. The results obtained using double-cysteine substitution mutants (Fig. 3) suggested that residues Ser^{52}, Ser^{151}, Ser^{313}, Ser^{485}, Ile^{605}, and Ser^{787} are also located at this interface. However, only two (S52C and S787C) of these mutants retained the enzyme activities. Therefore, residues Ser^{52} and Ser^{787} are the most likely candidates, in addition to Ser^{545}, for being at the interface between individual subunits. We need to perform high-resolution crystallographic studies, especially two-dimensional crystallography, to confirm the tertiary structure of H^+-PPases in the membrane.

Acknowledgements

This work was supported by Grants-in-Aid for Scientific Research 13142203 and 13CE2005 (to M.M.) from the Ministry of Education, Sports and Culture, Science and Technology of Japan.

References

[1] M. Maeshima, Vacuolar H^+-pyrophosphatase, Biochim. Biophys. Acta 1465 (2000) 37–51.
[2] M. Baltscheffsky, A. Schultz, H. Baltscheffsky, H^+-PPases: a tightly membrane-bound family, FEBS Lett. 457 (1999) 527–533.
[3] Y.M. Drozdowicz, P.A. Rea, Vacuolar H^+-pyrophosphatases: from the evolutionary backwaters into the mainstream, Trends Plant Sci. 6 (2001) 206–211.
[4] M. Maeshima, TONOPLAST TRANSPORTERS: organization and function, Annu. Rev. Plant Physiol. Plant Mol. Biol. 52 (2001) 469–497.
[5] Y. Nakanishi, T. Saijo, Y. Wada, M. Maeshima, Mutagenic analysis of functional residues in putative substrate-binding site and acidic domains of vacuolar H^+-pyrophosphatase, J. Biol. Chem. 276 (2001) 7654–7660.
[6] J.R. Pérez-Castiñeira, J. Alvar, L.M. Ruiz-Pérez, A. Serrano, Evidence for a wide occurrence of proton-translocating pyrophosphatase genes in parasitic and free-living protozoa, Biochem. Biophys. Res. Commun. 294 (2002) 567–573.
[7] M.T. McIntosh, A.B. Vaidya, Vacuolar type H^+ pumping pyrophosphatases of parasitic protozoa, Int. J. Parasitol. 32 (2002) 1–14.
[8] M. Baltscheffsky, S. Nadanaciva, A. Schultz, A pyrophosphate synthase gene: molecular cloning and sequencing of the cDNA encoding the inorganic pyrophosphate synthase from *Rhodospirillum rubrum*, Biochim. Biophys. Acta 1364 (1998) 301–306.
[9] L. Schocke, B. Schink, Membrane-bound proton-translocating pyrophosphatase of *Syntrophus gentianae*, a syntrophically benzoate-degrading fermenting bacterium, Eur. J. Biochem. 256 (1998) 589–594.
[10] J.R. Pérez-Castiñeira, R.L. López-Marqués, M. Losada, A. Serrano, A thermostable K^+-stimulated vacuolar-type pyrophosphatase from the hyperthermophilic bacterium *Thermotoga maritima*, FEBS Lett. 496 (2001) 6–11.
[11] Y.M. Drozdowicz, Y.P. Lu, V. Patel, S. Fitz-Gibbon, J.H. Miller, P.A. Rea, A thermostable vacuolar-type membrane pyrophosphatase from the archaeon *Pyrobaculum aerophilum*: implications for the origins of pyrophosphate-energized pumps, FEBS Lett. 460 (1999) 505–512.
[12] D.A. Scott, W. de Souza, M. Benchimol, L. Zhong, H.G. Lu, S.N. Moreno, R. Docampo, Presence of a plant-like proton-pumping pyrophosphatase in acidocalcisomes of *Trypanosoma cruzi*, J. Biol. Chem. 273 (1998) 22151–22158.
[13] M. Seufferheld, M.C. Vieira, F.A. Ruiz, C.O. Rodrigues, S.N. Moreno, R. Docampo, Identification of organelles in bacteria similar to acidocalcisomes of unicellular eukaryotes, J. Biol. Chem. 278 (2003) 29971–29978.
[14] L.S. Motta, W.S. da Silva, D.M. Oliveira, W. de Souza, E.A. Machado, A new model for proton pumping in animal cells: the role of pyrophosphate, Insect Biochem. Mol. Biol. 34 (2004) 19–27.
[15] R.L. López Marqués, J.R. Pérez Castiñeira, M. Losada, A. Serrano, Differential regulation of soluble and membrane-bound inorganic pyrophosphatases in the photosynthetic bacterium *Rhodospirillum rubrum* provides insights into pyrophosphate-based stress bioenergetics, J. Bacteriol. 186 (2004) 5418–5426.
[16] R. Garcia Contreras, H. Celis, I. Romero, Importance of *Rhodospirillum rubrum* H^+-pyrophosphatase under low-energy conditions, J. Bacteriol. 186 (2004) 6651–6655.

[17] A. Fukuda, K. Chiba, M. Maeda, A. Nakamura, M. Maeshima, Y. Tanaka, Effect of salt and osmotic stresses on the expression of genes for the vacuolar H^+-pyrophosphatase, H^+-ATPase subunit A, and Na^+/H^+ antiporter from barley, J. Exp. Bot. 55 (2004) 585–594.
[18] R.A. Gaxiola, R. Rao, A. Sherman, P. Grisafi, S.L. Alper, G.R. Fink, The *Arabidopsis thaliana* proton transporters, AtNhx1 and Avp1, can function in cation detoxification in yeast, Proc. Natl. Acad. Sci. U. S. A. 96 (1999) 1480–1485.
[19] R.A. Gaxiola, J. Li, S. Undurraga, L.M. Dang, G.J. Allen, S.L. Alper, G.R. Fink, Drought- and salt-tolerant plants result from overexpression of the AVP1 H^+-pump, Proc. Natl. Acad. Sci. U. S. A. 98 (2001) 11444–11449.
[20] M. Maeshima, H^+-translocating inorganic pyrophosphatase of plant vacuoles. Inhibition by Ca^{2+}, stabilization by Mg^{2+} and immunological comparison with other inorganic pyrophosphatases, Eur. J. Biochem. 196 (1991) 11–17.
[21] R. Gordon-Weeks, S.H. Steele, R.A. Leigh, The role of magnesium, pyrophosphate, and their complexes as substrates and activators of the vacuolar H^+-pumping inorganic pyrophosphatase (studies using ligand protection from covalent inhibitors), Plant Physiol. 111 (1996) 195–202.
[22] Y.M. Drozdowicz, J.C. Kissinger, P.A. Rea, AVP2, a sequence-divergent, K^+-insensitive H^+-translocating inorganic pyrophosphatase from Arabidopsis, Plant Physiol. 123 (2000) 353–362.
[23] E.J. Kim, R.G. Zhen, P.A. Rea, Site-directed mutagenesis of vacuolar H^+-pyrophosphatase. Necessity of Cys^{634} for inhibition by maleimides but not catalysis, J. Biol. Chem. 270 (1995) 2630–2635.
[24] R.G. Zhen, E.J. Kim, P.A. Rea, Acidic residues necessary for pyrophosphate-energized pumping and inhibition of the vacuolar H^+-pyrophosphatase by *N,N′*-dicyclohexylcarbodiimide, J. Biol. Chem. 272 (1997) 22340–22348.
[25] A. Takasu, Y. Nakanishi, T. Yamauchi, M. Maeshima, Analysis of the substrate binding site and carboxyl terminal region of vacuolar H^+-pyrophosphatase of mung bean with peptide antibodies, J. Biochem. 122 (1997) 883–889.
[26] G.A. Belogurov, M.V. Turkina, A. Penttinen, S. Huopalahti, A.A. Baykov, R. Lahti, H^+-pyrophosphatase of *Rhodospirillum rubrum*. High yield expression in *Escherichia coli* and identification of the Cys residues responsible for inactivation my mersalyl, J. Biol. Chem. 277 (2002) 22209–22214.
[27] A. Schultz, M. Baltscheffsky, Properties of mutated *Rhodospirillum rubrum* H^+-pyrophosphatase expressed in *Escherichia coli*, Biochim. Biophys. Acta 1607 (2003) 141–151.
[28] Y. Nakanishi, I. Yabe, M. Maeshima, Patch clamp analysis of a H^+ pump heterologously expressed in giant yeast vacuoles, J. Biochem. 134 (2003) 615–623.
[29] Y.Y. Hsiao, R.C. Van, S.H. Hung, H.H. Lin, R.L. Pan, Roles of histidine residues in plant vacuolar H^+-pyrophosphatase, Biochim. Biophys. Acta 1608 (2004) 190–199.
[30] A. Schultz, M. Baltscheffsky, Inhibition studies on *Rhodospirillum rubrum* H^+-pyrophosphatase expressed in *Escherichia coli*, Biochim. Biophys. Acta 1656 (2004) 156–165.
[31] G.A. Belogurov, R. Lahti, A lysine substitute for K^+. A460K mutation eliminates K^+ dependence in H^+-pyrophosphatase of *Carboxydothermus hydrogenoformans*, J. Biol. Chem. 277 (2002) 49651–49654.
[32] A.M. Malinen, G.A. Belogurov, M. Salminen, A.A. Baykov, R. Lahti, Elucidating the role of conserved glutamates in H^+-pyrophosphatase of *Rhodospirillum rubrum*, J. Biol. Chem. 279 (2004) 26811–26816.
[33] H. Mimura, Y. Nakanishi, M. Hirono, M. Maeshima, Membrane topology of the H^+-pyrophosphatase of *Streptomyces coelicolor* determined by cysteine-scanning mutagenesis, J. Biol. Chem. 279 (2004) 35106–35112.
[34] M. Maeshima, Oligomeric structure of H^+-translocating inorganic pyrophosphatase of plant vacuoles, Biochem. Biophys. Res. Commun. 168 (1990) 1157–1162.
[35] M.H. Sato, M. Maeshima, Y. Ohsumi, M. Yoshida, Dimeric structure of H^+-translocating pyrophosphatase from pumpkin vacuolar membranes, FEBS Lett. 290 (1991) 177–180.
[36] C.M. Tzeng, C.Y. Yang, S.J. Yang, S.S. Jiang, S.Y. Kuo, S.H. Hung, J.T. Ma, R.L. Pan, Subunit structure of vacuolar proton-pyrophosphatase as determined by radiation inactivation, Biochem. J. 316 (1996) 143–147.
[37] V. Sarafian, M. Potier, R.J. Poole, Radiation-inactivation analysis of vacuolar H^+-ATPase and H^+-pyrophosphatase from *Beta vulgaris* L. Functional sizes for substrate hydrolysis and for H^+ transport, Biochem. J. 283 (1992) 493–497.
[38] S.J. Yang, S.J. Ko, Y.R. Tsai, S.S. Jiang, S.Y. Kuo, S.H. Hung, R.L. Pan, Subunit interaction of vacuolar H^+-pyrophosphatase as determined by high hydrostatic pressure, Biochem. J. 331 (1998) 395–402.
[39] S.J. Yang, S.S. Jiang, Y.Y. Hsiao, R.C. Van, Y.J. Pan, R.L. Pan, Thermo-inactivation analysis of vacuolar H^+-pyrophosphatase, Biochim. Biophys. Acta 1656 (2004) 88–95.
[40] L. Galili, K. Herz, O. Dym, E. Padan, Unraveling functional and structural interactions between transmembrane domains IV and XI of NhaA Na^+/H^+ antiporter of *Escherichia coli*, J. Biol. Chem. 279 (2004) 23104–23113.
[41] T. Hisamitsu, T. Pang, M. Shigekawa, S. Wakabayashi, Dimeric interaction between the cytoplasmic domains of the Na^+/H^+ exchanger NHE1 revealed by symmetrical intermolecular cross-linking and selective co-immunoprecipitation, Biochemistry 43 (2004) 11135–11143.
[42] Y. Kubo, S. Konishi, T. Kawabe, S. Nada, A. Yamaguchi, Proximity of periplasmic loops in the metal-Tetracycline/H^+ antiporter of *Escherichia coli* observed on site-directed chemical cross-linking, J. Biol. Chem. 275 (2000) 5270–5274.
[43] N. Ermolova, L. Guan, H.R. Kaback, Intermolecular thiol cross-linking via loops in the lactose permease of *Escherichia coli*, Proc. Natl. Acad. Sci. U. S. A. 100 (2003) 10187–10192.
[44] B.A. van Montfort, G.K. Schuurman Wolters, J. Wind, J. Broos, G.T. Robillard, B. Poolman, Mapping of the dimer interface of the *Escherichia coli* mannitol permease by cysteine cross-linking, J. Biol. Chem. 277 (2002) 14717–14723.
[45] M. Soskine, S. Steiner Mordoch, S. Schuldiner, Crosslinking of membrane-embedded cysteines reveals contact points in the EmrE oligomer, Proc. Natl. Acad. Sci. U. S. A. 99 (2002) 12043–12048.
[46] T.W. Loo, M.C. Bartlett, D.M. Clarke, Disulfide cross-linking analysis shows that transmembrane segments 5 and 8 of human P-glycoprotein are close together on the cytoplasmic side of the membrane, J. Biol. Chem. 279 (2004) 7692–7697.
[47] R.D. Kirsch, E. Joly, An improved PCR-mutagenesis strategy for two-site mutagenesis or sequence swapping between related genes, Nucleic Acids Res. 26 (1998) 1848–1850.
[48] C. Toyoshima, H. Nomura, Structural changes in the calcium pump accompanying the dissociation of calcium, Nature (London) 418 (2002) 605–611.
[49] Y. Gerchman, A. Rimon, M. Venturi, E. Padan, Oligomerization of NhaA, the Na^+/H^+ antiporter of *Escherichia coli* in the membrane and its functional and structural consequences, Biochemistry 40 (2001) 3403–3412.
[50] F. Kilic, G. Rudnick, Oligomerization of serotonin transporter and its functional consequences, Proc. Natl. Acad. Sci. U. S. A. 97 (2000) 3106–3111.
[51] U. Ludewig, S. Wilken, B. Wu, W. Jost, P. Obrdlik, M. El Bakkoury, A.M. Marini, B. Andre, T. Hamacher, E. Boles, N. von Wiren, W.B. Frommer, Homo- and hetero-oligomerization of ammonium transporter-1 NH_4^+ uniporters, J. Biol. Chem. 278 (2003) 45603–45610.
[52] M. Maeshima, S. Yoshida, Purification and properties of vacuolar membrane proton-translocating inorganic pyrophosphatase from mung bean, J. Biol. Chem. 264 (1989) 20068–20073.